Effect of Viscosities on the Spray Characteristics of Pressure Swirl Nozzle

Z. M. Liu[†], J. Y. Lin, H. L. Zheng and Y. Pang

College of Mechanical Engineering and Applied Electronics Technology, Beijing University of Technology, Beijing 100124, China

†*Corresponding Author Email: lzm@bjut.edu.cn*

ABSTRACT

The effects of medium viscosity on the spray flow rate, spray Sauter Mean Diameter, droplet velocity and spray cone angle of pressure swirl nozzles are investigated by making use of the particle dynamics analysis system and high-speed photographic system. Based on the axial and radial distribution characteristics of Sauter Mean Diameter and droplet velocity, the water-glycerol mixture is used to simulate medium with a wide range of viscosities. It is found that with the increase of viscosity, the turbulence of the medium flow and the swirling effect is weakened, and the rated pressure becomes larger and the spray flow rate increases. Spray Sauter Mean Diameter and droplet axial velocity becomes larger, while the spray cone angle decreases. The development of the axial velocity distribution of spray cone is characterized by the radial and axial position parameters. The area of the large-droplet region on both sides of spray cone becomes larger, and the area of small-droplet region near the axis becomes smaller.

Keywords: PDA system; Spray characteristics; SMD; Spray cone angle; Medium viscosity.

NOMENCLATURE

sC_1	an empirical coefficient associated with the nozzle structure		liquid
		V	volumetric flow of the medium
C_2	the constant	We	Weber number
C_d	the discharge coefficient		
D_{max}	the maximum stable diameter	μ	viscosity of the medium
P	pressure	σ	surface tension of spray medium
r_0	radius near the exit of the nozzle	ρ_g	the ambient gas density
r_c	radius of the air core near the orifice		
Re	Reynolds Number	ρ_l	the ambient medium density
SMD	Sauter Mean Diameter		
v	relative velocity difference of gas and		

1. INTRODUCTION

As a key component of the combustion chamber of aero engine, the fuel nozzle realizes the fuel atomization. (Liu *et al*. 2013) The spray characteristics directly determine the combustion performance and pollutant emission of the engine. Compared with the traditional method (Pang *et al*. 2014; Wang *et al*. 2017) of droplet generation, pressure swirl nozzles are widely used in rocket engines, aero engines, gas turbines and other power equipment (Xie *et al*. 2013)

because of its geometrical simplicity, good atomization performance and low cost. The viscosity of spray medium has an important influence on the spray characteristics of the pressure swirl nozzle (Wang *et al*. 2013; Chen *et al*. 2015). Studying on the effect of the medium viscosity on the atomization effect of the nozzle deeply can not only improve the atomization quality and the nozzle design criteria, but also provide theoretical basis on finding a substitute for fossil fuel (Fan *et al*. 2014; Hashimoto *et al*. 2014; Davanlou *et al*. 2015).

The Sauter Mean Diameter (SMD) of spray cone is an important indicator for evaluating the spray characteristics of the pressure swirl nozzle. Overlarge SMD will cause combustion efficiency decreasing and carbon deposition increasing. Meanwhile, droplet with small SMD will be taken away by the airflow and cannot be evenly distributed well in the combustion chamber, which results in unstable combustion (Hashimoto *et al.* 2014). Studies (Lee *et al.* 2010; Hashimoto *et al.* 2014, Amini 2016) have shown that, high medium viscosity will make the spray SMD increase (Moon *et al.* 2007; Lee *et al.* 2010; Fan *et al.* 2014). Lee *et al.* (2010) and Moon (2007) found that the high medium viscosity will reduce the diameter of air core, resulting in the increase of the liquid film thickness and the spray SMD. Kim *et al.* (2017) found that mean diameter of the particles is proportional to the viscosity of the slurry. Fan *et al.* (2014) and Dafsari *et al.* (2019) indicated that with the increase of viscosity, the unfolded liquid film will show five different forms (from the smooth to the wrinkled). High viscosity will reduce the turbulence of the flow and the breakup of the liquid film, which makes the spray SMD increase. Sun *et al.* (2018) revealed that the SMD near the orifice is small because turbulence kinetic energy of air near the orifice is maximum. The spray cone angles reflect the distribution of the droplets in the combustion chamber. Small spray cone angle makes the droplets pass through the turbulent airflow region resulting in the low mixing efficiency, which reduces combustion efficiency. Also, the wall surface will be overheated and produces carbon deposition. If the spray cone angle is too small, the droplets cannot be effectively distributed to the entire combustion chamber, which makes combustion efficiency decline (Liu *et al.* 2013; Davanlou *et al.* 2015). Therefore, forming spray cone angle that matches the size of combustion chamber has an important impact on the combustion process. Zhang *et al.* (1989) theoretically derived the empirical formula of the spray cone angle of the pressure swirl nozzle, and verified the accuracy of the formula through experiments. Mohammad *et al.* (2010) disclosed that with increasing the power-law index the spray cone angle decreases and the discharge coefficient increases. Dacanlou *et al.* (2015) and Wen *et al.* (2016) found that the spray cone angle decreases as the viscosity of the medium increases. Different medium viscosity can also change the flow characteristics of the nozzle. Chung *et al.* (1998) and Wimmer *et al.* (2013) found that the Spray Flow Rate (SFR) increases with the increase of the medium viscosity. Lee *et al.* (2010) supposed that the phenomenon is due to the fact that high medium viscosity causes the diameter of the air core to decrease.

Most of the existing investigations focus on the influence of medium viscosity on the SMD and liquid film breakup process of the pressure swirl nozzle, while the study on the effect of the medium viscosity on the droplet size distribution

and velocity distribution is less. Only using the droplet average diameter and the axial velocity is not enough to fully evaluate the atomization quality and indicate the atomization characteristics. It is necessary to measure and control the particle size and velocity distribution of the whole spray cone (Liu *et al.* 2018; Liu *et al.* 2018), so that the medium can be mixed with the air better and the combustion efficiency is improved. Therefore, this paper details the PDA experiment carried out to deeply investigate the SFR, the spray SMD, the axial velocity of the droplet and the spray cone angle of the pressure swirl nozzle under different medium viscosity conditions, to get the corresponding rated pressure under different viscosity conditions. The flow characteristics of the droplets inside the spray cone under the rated pressure are analyzed. The effect of the medium viscosity on the spray SMD, the axial velocity of the droplet, the spray cone angle, the velocity distribution and the droplet size distribution are investigated.

2. EXPERIMENTAL DESIGN

2.1 Experimental Apparatus

Photographic and schematic diagram of experimental apparatus used in this study are shown in Fig. 1. It consists of an experimental nozzle, a dynamic particle analyzer, a high-speed camera system, and a supply system.
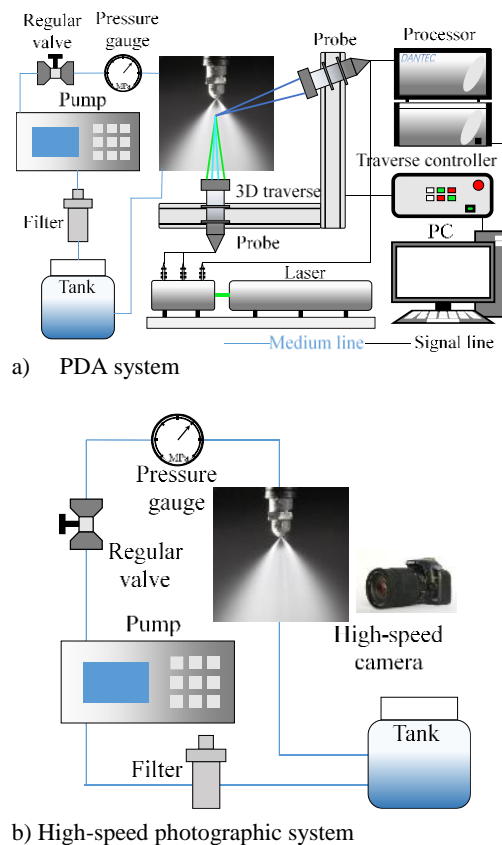

a) PDA system

b) High-speed photographic system
Fig. 1. Schematic diagram of experimental device.

The supply system is shown in Fig. 1-a). The medium in the water tank enters the pipeline through a filter, a constant flow pump (LP0110, Shanghai Sanwei Technology), and is finally ejected through the experimental nozzle. The regulator valve (DN20, Shanghai Qiaoshi) can make the output pressure of the constant flow pump more stable and reduce the pulsation error. The pressure gauge (HSFN-60, Hangzhou Kechuang) can measure the spray pressure difference during the spraying process, and the range of pressure gauge is 0-1.6 MPa.

The 3D Dynamic Particle Test and Analysis System (3D Fiber PDA, Dantec) are shown in Fig. 1-a), which can directly measure the velocity and droplet size distribution of the spray cone.

The high-speed photo shooting system is shown in Fig. 1-b), with a digital camera (5D2, Canon) equipped with an EF 70-200mm f/4L IS USM lens to shoot the spray cone, to measure the spray cone angle.

2.2 Nozzle Configuration

The experimental nozzle structure used in this paper is shown in Figs. 2 and 3. The specific structural parameters are shown in Table 1. The atomizer is composed of an inlet section, an acceleration section, a swirling section and an orifice. The medium enters the nozzle from the inlet section and accelerates in the acceleration section. When it passes through the swirling section, medium is forced to follow a helical path. The high-speed rotating medium forms a negative pressure zone near the rotating shaft which can attract ambient air. The air core is formed into the swirling chamber, and it presses medium near the orifice to form a liquid film, which emerges from the orifice and breaks up into a cluster of thin sheet.
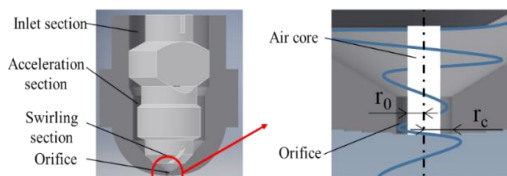

Fig. 2. Structure of experimental nozzle.

Fig. 3. Schematic diagram of experimental nozzle.

Table 1 Size parameters of the experimental nozzle

Structure	Parameter
swirl trough lift angle/°	45
swirl trough number	3
swirl trough depth/μm	900
swirl trough width/μm	600
orifice width/μm	800

2.3 Nozzle Configuration

In this paper, the medium viscosity is changed by the method of Chung *et al*. (1998). 10wt%, 30wt%, and 50wt% water-glycerin mixtures are used to simulate the actual operating conditions. All experiments are carried out at room temperature (20 ℃). The viscosity of the three mass fractions of the glycerin-water mixture at room temperature is shown in Table 2, and the viscosity is measured by the rheometer (R/S Plus, Brookfield).

Table 2 Viscosity of the three media at room temperature (20℃)

Serial number	Spray medium	Viscosity（mPa·s）
A	10wt% water-glycerin mixtures	1.31
B	30wt% water-glycerin mixtures	2.5
C	50wt% water-glycerin mixtures	6

3. RESULTS AND DISCUSSION

3.1 Effect of Medium Viscosity on Spray Cone Angle

The spray cone angle can indicate the degree of droplet dispersion. The spray morphology of medium A, B and C under the pressure of 0.08MPa~0.30MPa is shown in Fig. 4.

The spray cone angle is defined as the angle between the two gas-liquid border lines near the orifice. In order to improve the accuracy of spray cone angle measurement, this paper adopts the image processing method of Kang *et al* (2014). First, the captured images are converted into grayscale images by MATLAB. Then grayscale image is binarized to determine border lines used to measure the spray cone angle. As shown in Fig. 4, the spray development of three media is generally similar.

After the spray medium passes through the swirling section, it rotates in the swirl chamber and emerges from the orifice in the form of liquid film. When the pressure is low (the pressure of medium A and B are less than 0.10 MPa and the pressure of medium C is less than 0.12 MPa), the SFR of medium is slow, and the liquid film has a tendency to expand by its own inertia. However, the surface tension eventually overcomes it, and the conical liquid film does not break and shrink into a hollow bubble.
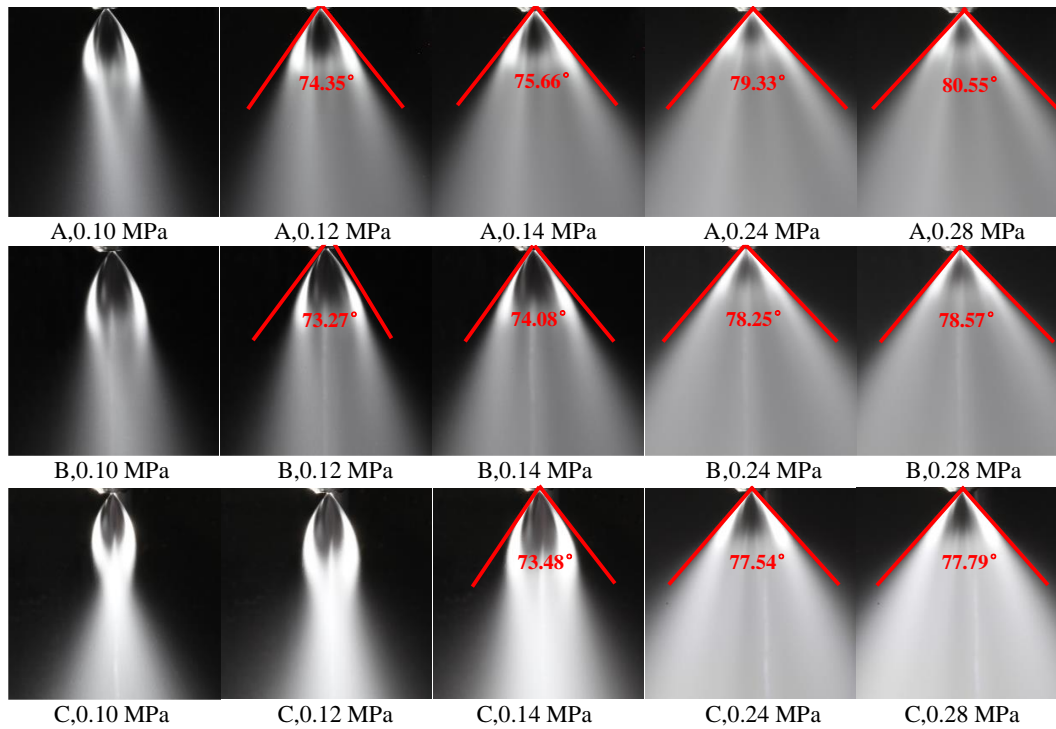
Fig. 4. Spray morphology.

Large droplets are formed downstream of the bubble. As the pressure and the medium SFR increases, the surface tension cannot overcome the inertia of the liquid film, and the liquid film continues to expand outward. The spray cone gradually becomes larger, and the variation of the spray cone angle is shown in Fig. 5. When the pressure increases from 0.12 MPa to 0.28 MPa, the spray cone angles of medium A and medium B increase from 74.35° and 73.27° to 80.58° and 78.58°, and finally keep stable at 80.6° and 78.6°; When the pressure increases from 0.14 MPa to 0.24 MPa, the spray cone angle of the medium C increases from 73.48° to 77.79°, and finally keeps stable at 78.8°. When the pressure reaches a certain value (the pressure of medium A is greater than 0.28 MPa and the pressure of medium B and C is greater than 0.24 MPa), the internal friction loss of the nozzle increases as the tangential speed increases.
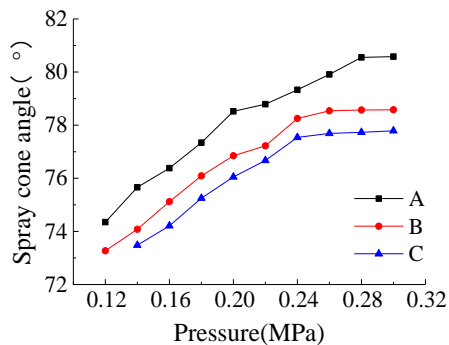

Fig. 5. Curves of pressure versus spray cone angle.

The spray cone angle does not change as the pressure increases. Under the same pressure, the spray cone angle decreases with the increase of viscosity, because the increase of the medium viscosity leads to the increase of the internal flow resistance of the nozzle, and the swirling effect is weakened. This result is consistent with the trend of the literature (Zhang *et al*. 1989; Dopazo *et al*. 1994; Wang *et al*. 2013).

3.2 Effect of Medium Viscosity on Flow Characteristics

The flow characteristics of the nozzle are important parameters of the nozzle performance and are mainly used for engine operating condition adjustment. The relationship between the SFR of the nozzle and pressure under different medium viscosity conditions is shown in Fig. 6. When the pressure is increased from 0.08 MPa to 0.44 MPa, the SFR of three media increases by 119.08%, 112.03%, and 111.18%, respectively. Under the same pressure condition, the flow characteristics increase with the increasing of viscosity. When the viscosity rises up from 1.12 mPa·s to 3.26 mPa·s and the pressure rises up from 0.08 MPa to 0.44 MPa, the SFR increases by 11.8%. Fu *et al*. (2011) gives this phenomenon an explanation. Equation (1) is an empirical formula for the radius of the air core near the orifice of the pressure swirl nozzle given by Fu *et al*. (2011). As μ increases, r_c decreases, which indicates that the radius of the air core reduces. As a result, both the flow area near the orifice and the flow characteristics increase. Meanwhile, r_c is proportional to $\mu^{0.25}$, so when the viscosity grows up from 1.31 mPa·s to 2.5 mPa·s, there is a smaller increase in the SFR. However,

when from 2.5 mPa·s to 6 mPa·s, the SFR grows up.

$$r_c = r_0 - C_1 \left(\frac{2r_0 V \mu}{\Delta P} \right)^{0.25} \qquad (1)$$

where r_c is the radius of the air core near the orifice, r_0 is the radius near the exit of the nozzle, V is the volumetric flow of the medium, μ is the viscosity of the medium, ΔP is the pressure, and C_1 is the empirical coefficient associated with the nozzle structure.
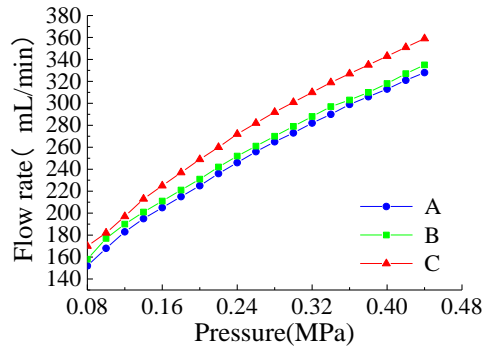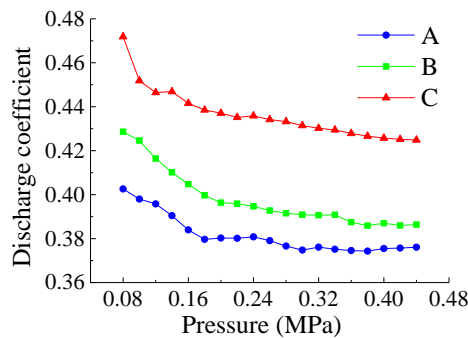

Fig. 6. Curves of pressure versus flow rate.

Fig. 7. Curves of pressure versus discharge coefficient.

Figure 7 illustrates the discharge coefficient of media with different viscosities. Discharge coefficient (C_d) is defined as Equ (2), where ρ_l is the medium density. It is seen that the discharge coefficient decreases with the increase of the pressure from 0.08 MPa to 0.46 MPa, however it tends to be stable under high pressure condition. Meanwhile, the discharge coefficient declines with the growth of the medium viscosity.

$$C_d = \frac{V}{\pi r_0^2 \square \sqrt{2\Delta P / \rho_l}} \qquad (2)$$

3.3 Effect of Medium Viscosity on Spray SMD and Axial Velocity

Spray SMD and axial velocity are measured at the spray center 50 mm below the orifice. The relationship between SMD and pressure under different medium viscosity conditions is shown in Fig. 8. As the pressure increases, the SMD decreases and then tends to be gentle. The reason is that in the swirl chamber, the medium rotation

velocity increases as the pressure increases, leading to the swirl effect increasing. The diameter of the air core grows up, which makes liquid film thinner and broken more easily (Lee *et al.* 2010; Fu *et al.* 2011). When the pressure exceeds 0.36 MPa, 0.40 MPa, and 0.46 MPa respectively, the SMD reduction rate slows down and finally the spray SMD decreases to 29 μm, 32 μm, and 54 μm. Under the same pressure condition, the increase of viscosity will increase the SMD, because that the high medium viscosity will reduce the Reynolds number (*Re*) calculated by Eq. (3) and Eq. (4) (Fig. 9), and slow down the development of turbulence and the liquid film breakup (Wen *et al.* 2016).

$$v = \sqrt{\frac{2\Delta P}{\rho}} \qquad (3)$$
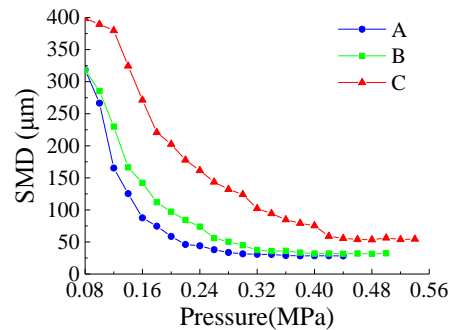
$$Re = \frac{\rho v l}{\mu} \qquad (4)$$

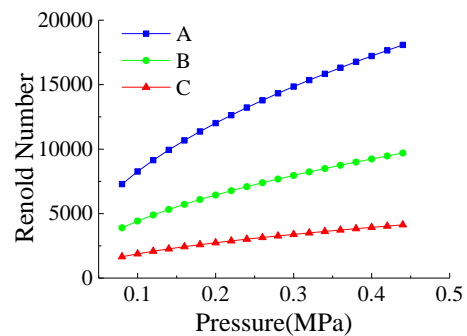**Fig. 8. Curves of pressure versus SMD.**

Fig. 9. Curves of pressure versus SMD.

The curves of droplet axial velocity with pressure under different medium viscosity conditions are shown in Fig. 10. As the pressure increases, the droplet axial velocity first decreases, and then increases, and finally tends to be gentle, because the droplet axial velocity is affected by both the pressure and the air suction The high-speed rotation of the medium in the swirl chamber creates a negative pressure zone at the nozzle axis, which sucks the droplets and slows down the droplet axial velocity (Fig. 11). As the pressure increases, the kinetic energy of the medium continues to increase and the axial velocity becomes larger. When the pressure exceeds 0.36 MPa, 0.40 MPa and 0.46 MPa, the axial velocity of the droplets tends to be gentle, reaching 5.8 m/s, 6.7 m/s and 8.3 m/s, respectively.
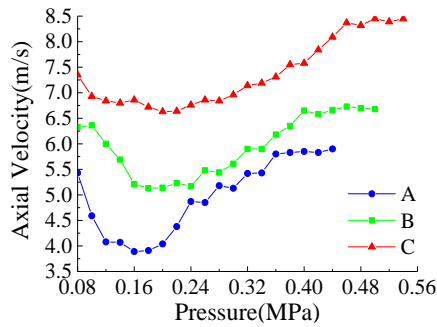
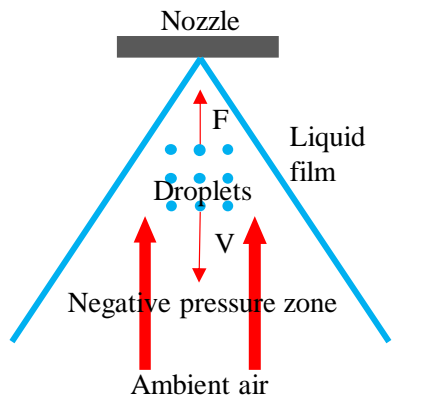**Fig. 10. Curves of pressure versus axial velocity.**

Fig. 11. Schematic diagram of the movement of droplet at the axis. The droplets in the negative pressure zone are sucked by the ambient air carried by the negative pressure （Suction F） and then slow down.

It is known from the droplet breakup mechanism in the steady gas flow that the droplet size decreases as the velocity difference between medium and ambient air increases. When the velocity differences do not change with the increase of the pressure, the droplets no longer break up basically. After the rated pressure is exceeded, the spray SMD and the droplet axial velocity tend to be stable, but the SFR continues to increase (Fig. 6), indicating that the number of droplets in the spray cone increases, but the flow state of the spray cone does not change. At the same pressure, the increase of viscosity results in the increase of droplet axial velocity due to the fact that high viscosity results in larger SMD, and the kinetic energy carried by a single droplet increases.

3.4 Effect of Medium Viscosity on Velocity Distribution Under Rated Pressure

Equations are centered and numbered consecutively, with equation numbers in parentheses flush right, as in Eq. (1). Insert a blank line on either side of the equation. First use the equation editor to create the equation.

In order to make the combustion steady, the spray cone should be stabilized. Due to the advantage of low rated pressure of the pressure swirl nozzle, the spray cone can be stable under various working conditions (García *et al.* 2016), so the rated pressure conditions are chosen as typical conditions to be investigated. As can be seen from Sections 2.1 to

2.3, when the pressure is 0.46 MPa, the atomization of three different media reaches the rated pressure. The measurement area is shown in Fig 12. Spray measurements are carried out by 16 axial stations taken from 10 mm to 80 mm below the nozzle and every 5 mm along the axial direction. The spray SMD and droplet velocity are measured every 2 mm in the radial direction of each axial station until the radial boundary of spray cone. The left half area of droplets is measured, and the right half is directly obtained according to the symmetry (Santolaya *et al.* 2010).

Fig. 12. Schematic diagram of measurement area.

In order to study the axial and radial distribution of the droplet axial, the measured points are interpolated using Tecplot software to obtain the axial velocity contours and streamline diagram of the central section of the spray cone at different viscosities shown in Fig. 13 and Fig. 14. The axial velocity curves of axial distances of 20 mm, 40 mm, 60 mm, and 80 mm, respectively, are shown in Fig. 15. The axial velocity at the section of 10 mm to 20 mm below the nozzle shows obviously "double peak distribution" which means high velocity on both sides but low in the middle. (Fig. 13, Fig. 15). The axial velocity of expansion direction of the liquid film is high and the maximum velocity reaches 17.21 m/s, 16.56 m/s, and 15.53 m/s respectively. The velocity gradient of small droplets breaking up from the liquid film is high, due to the shearing action with the central air core, and the velocity decays faster. Velocity of the middle part is low because the swirling effect of the nozzle causes a negative pressure zone formed at the axis. The negative pressure zone will suck the internal droplets, leading to the velocity drop, and some small droplets even flows back. (Fig 14). As the viscosity increases, the swirling effect gradually decreases, and the area of the low velocity zone becomes smaller. At 20 mm to 30 mm below the nozzle, droplets are gradually slowed down by the ambient air. When the circumferential velocity of droplets around the air core is not enough to support the central negative pressure, the air core will collapse and droplets near the air core will move to the axis, forming a "densest spray region" at the axis of the spray

cone (Santolaya *et al.* 2010) (Fig. 15). The ambient air enters the spray cone to compensate the corresponding volume, and the incoming air is on both sides of the "densest spray region" and causes the medium to slow down. (Fig. 12 and Fig. 14) The radial distribution of the axial velocity gradually changes from "double peak distribution" to "triple peak distribution" (Fig. 14), which is consistent with the conclusion of literature (Santolaya *et al.* 2010; Durdina *et al.* 2014).
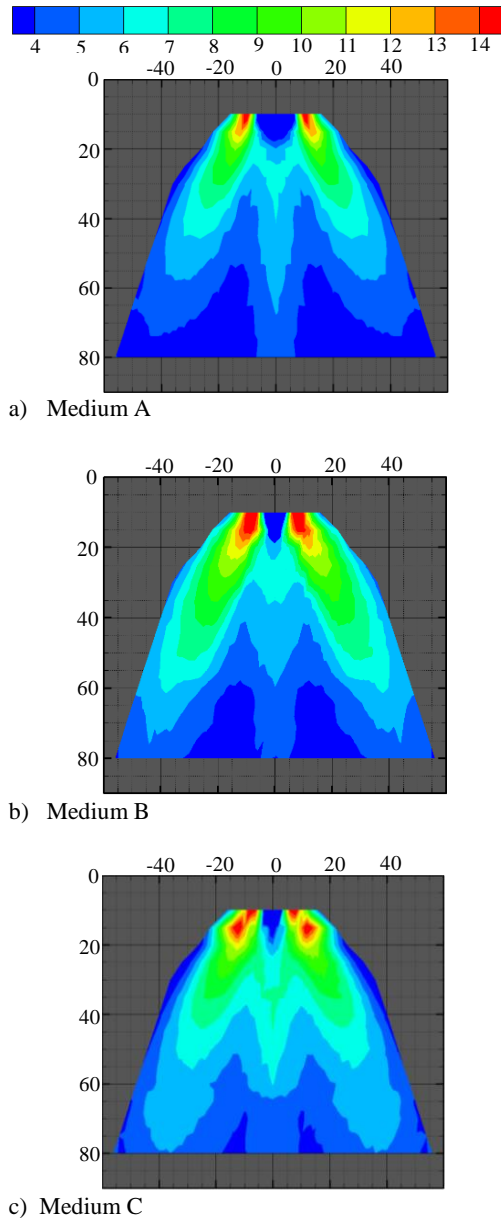

a)   Medium A

b)   Medium B

c)   Medium C

Fig. 13 Axial velocity contours of the center section of the spray cone.

As shown in Fig. 13-a), the velocity gradient along the expansion direction of the liquid film is high, but in "densest spray region" is low. So, the spray cone eventually develops to a "single peak distribution". As the viscosity increases, the spray SMD and the axial velocity becomes larger, resulting in the spray distance increasing. Distance

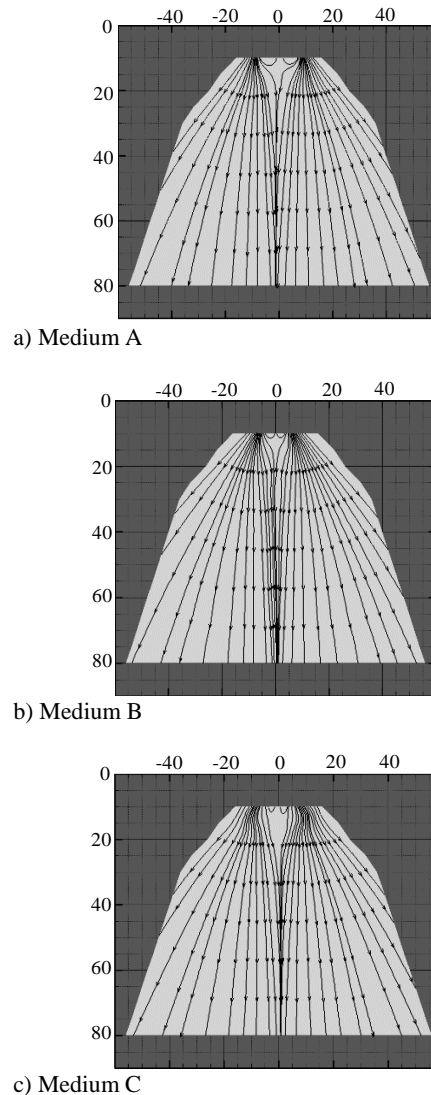that the spray cone reaches a fully development also rises up.

a) Medium A

b) Medium B

c) Medium C

Fig. 14 Streamline diagram of the center of spray cone.

3.5 Effect of Medium Viscosity on SMD Distribution under Rated Pressure

Under the condition of pressure of 0.46 MPa, the axial and radial distribution of droplet SMD at different viscosities are shown in Fig. 17 and Fig. 18 (the color and size of the dots all represent the SMD). It can be seen that the SMD distribution is generally similar, and can be divided into three regions according to the droplet SMD. The droplet SMD in the region I is larger than 110 μm, region II from 50 μm to 110 μm, and region III less than 50 μm. The droplet SMD is smaller as droplets are closer to the axis. The reason is that there is an air core near the center of the spray cone as shown in Fig. 3, which reduces the effective flow area of the medium. The medium is mainly concentrated around the air core where the gas-liquid shearing action happens. According to the Weber Criterion (Eq. 5), droplets are small due to the high velocity

difference at the gas-liquid interface, and this part of droplets moves to the "densest spray region" to form the region III after the air core collapses. In the middle part of the liquid film is far from the air core, resulting in the gas-liquid velocity difference being low and the droplet SMD getting larger. The rotation radius of this part of the droplet around the axis is different due to its own inertia. The larger the droplets become, the larger rotation radius of droplets is. The region I and the region II are formed by this part of droplets. As the medium viscosity increases, both the swirling effect and the number of small droplets decreases. The number of droplets with large particle size increases. The boundary line of the three regions moves toward the axis. The area of region III gets small, and the area of region I gets larger.
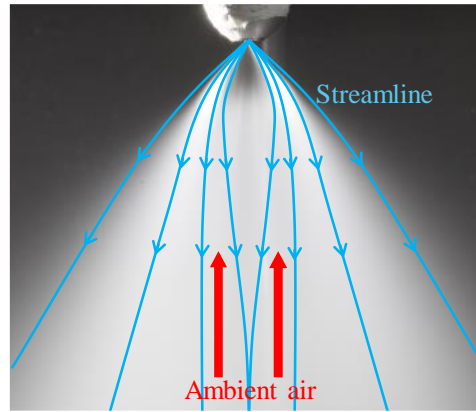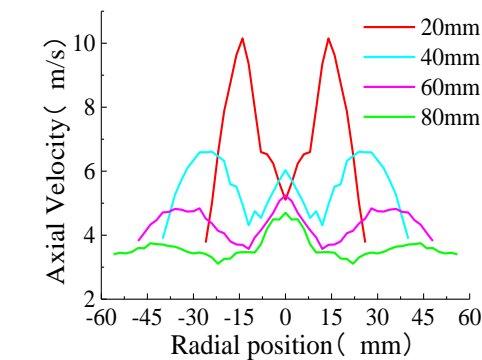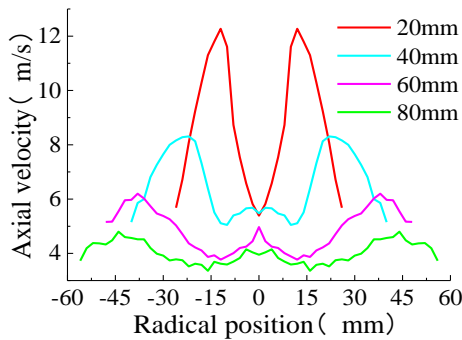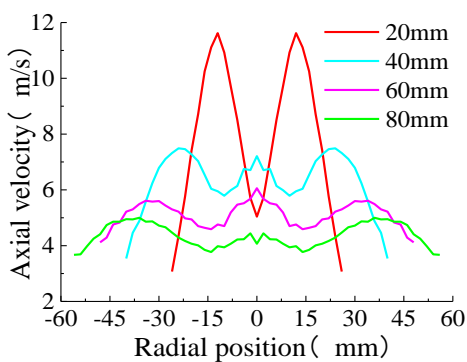

Fig. 16. Flow diagram in the spray cone.
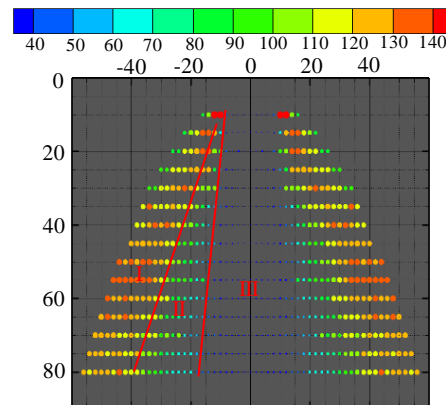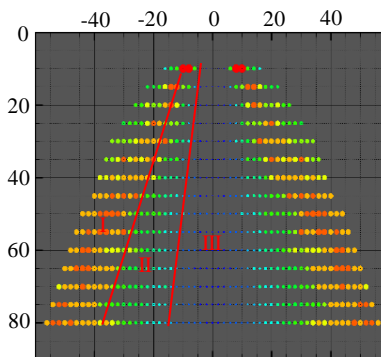

a) Medium A

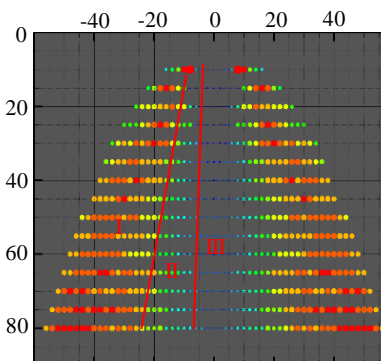b) Medium B

c) Medium C

Fig. 15. Curves of axial velocity-radial distribution of the central section of spray cone.

a) Medium A

b) Medium B

c) Medium C

Fig. 17. SMD-radial position profile. The spray cone is divided into three regions according to the droplet SMD.
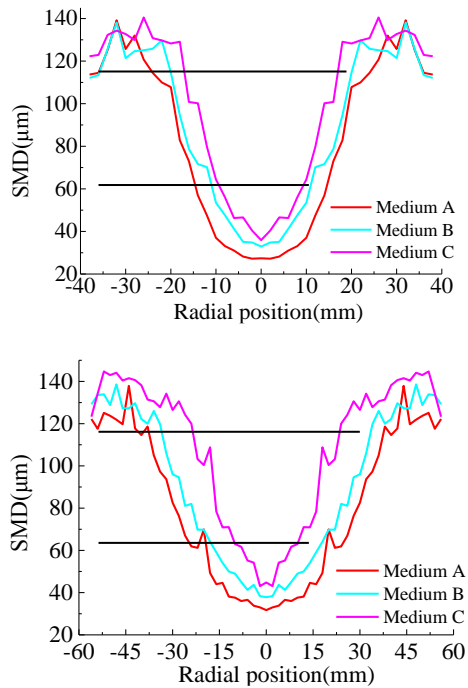
Fig. 18. SMD-radial position profile of different axial positions. a) The distribution curve of the SMD and radial position at the axial position of 40mm b) The distribution curve of the SMD and radial position at the axial position of 80mm.

$$D_{max} = \frac{W_e \sigma}{C_d \rho_g v^2} \tag{5}$$

where D_{max} is the maximum stable diameter, We is the Weber number, σ is the surface tension of spray medium, C_D is the constant, ρ_g is the ambient gas density, and v is the relative velocity difference of the gas and liquid.

4. CONCLUSION

The effect of medium viscosity on the spray characteristics of pressure swirl nozzle is experimentally studied. As the medium viscosity increases, the internal flow resistance of the nozzle increases, and the spray cone angle gradually decreases under the same pressure condition. Under the pressure of 0.08 MPa to 0.50 MPa, the spray cone angle of the medium C is between 1.8 and 2.2 degrees smaller than that of the medium A. At the same time, high viscosity causes Re number to decline, indicating that the spray turbulence and the swirling effect are weakened. The size of the air core reduces, resulting in flow characteristics, spray SMD, droplet axial velocity and rated pressure growing up. Under the condition of rated pressure, axial velocity distribution of spray cone changes from "double peak distribution", "triple peak distribution" to "single peak distribution". As the viscosity rises up, the area of the negative pressure zone below the nozzle gradually becomes small, but the spray distance and the distance that the spray cone forms a fully developed flow becomes longer. The area of the large-droplet region on both sides of spray cone rises up, and the area of small-droplet

region near the axis goes down.

REFERENCES

Amini, G (2016) Liquid flow in a simplex swirl nozzle. *International, Journal of Multiphase Flow* 79, 225.

Chen, L., Z. Liu, P. Sun and W. Huo (2015) Formulation of a fuel spray SMD model at atmospheric pressure using Design of Experiments (DoE), *Fuel* 153, 355-360.

Chung, I. P., C. Presser (1998) Effect of fluid Viscosity and Surface Tension on Liquid Sheet Disintegration of a Simplex Pressure-Swirl Atomizer. *Conference on Liquid Atomization and Spray Systems.*

Dafsari, R. A., H. J. Lee, J. Han, D. Park and J. Lee (2019) Viscosity effect on the pressure swirl atomization of an alternative aviation fuel, *Fuel* 240, 179-191

Davanlou, A., J. D. Lee, S. Basu and R. Kumar (2015) Effect of viscosity and surface tension on breakup and coalescence of bicomponent sprays. *Chemical Engineering Science* 131, 243-255.

Dopazo, C., J. Ballester (1994) Discharge Coefficient and Spray Angle Measurements for Small Pressure-Swirl Nozzles. *Atomization & Sprays* 4(3), 351-367.

Durdina, L., J. Jedelsky, M. Jicha (2014) Investigation and comparison of spray characteristics of pressure-swirl atomizers for a small-sized aircraft turbine engine. *International Journal of Heat & Mass Transfer* 78(7), 892-900.

Fan, Y., N. Hashimoto, H. Nishida and Y. Ozawa (2014) Spray characterization of an air-assist pressure-swirl atomizer injecting high-viscosity Jatropha oils, *Fuel* 121(2), 271-283.

Fu, Q. F., L. J. Yang and Qu, Y. Y. (2011) Measurement of annular liquid film thickness in an open-end swirl injector. *Aerospace Science & Technology* 15(2), 117-124.

García, J. A., J. L. Santolaya, A. Lozano, F. Barreras and E. Calvo (2016) Experimental characterization of the viscous liquid sprays generated by a Venturi-vortex atomizer. *Chemical Engineering & Processing Process Intensification* 105, 117-124.

Hashimoto, N., H. Nishida, Y. Ozawa (2014) Fundamental combustion characteristics of Jatropha oil as alternative fuel for gas turbines. *Fuel* 126(126), 194-201.

Kang, Z. T., Q. L. Li, X. Q. Zhang and P. Cheng (2014) Gas-liquid coaxial double centrifugal nozzle spray characteristics. *Journal of National University of Defense Technology* (5), 50-57.

Kim, H., T. Ko, S. Kim and W. Yoon (2017) Spray characteristics of aluminized-gel fuels sprayed using pressure-swirl atomizer. *Journal of Non-Newtonian Fluid Mechanics* 249, 36-47

Lee, E. J., Y. O. Sang, H. Y. Kim, S. C. James and S. S. Yoon (2010) Measuring air core characteristics of a pressure-swirl atomizer via a transparent acrylic nozzle at various Reynolds numbers. *Experimental Thermal & Fluid Science* 34(8), 1475-1483.

Liu, C. X., F. Q. Liu, Y. H. Mao, Y. Mu and G. Xu (2013) Experimental study on fuel space distribution characteristics of centrifugal nozzles for a certain type of aero engine, *Journal of Aerospace Power* 28(4), 783-791.

Liu, Z. M., K. F. Wang, Z. L. Wang, H. L. Zheng, T. Zhang and Z. Y. Kang (2018) Effect of stepped acceleration section on atomization characteristics of swirl nozzle. *Chinese Journal of Theoretical and Applied Mechanics* 50(3), 570-578.

Liu, Z. M., Z. L. Wang, K. F. Wang, et al. (2018b) Influences of dorsal pressure difference on the atomization performance of a pressure swirl nozzle. *Journal of Beijing University of Technology* 44(8), 1063-1068.

Mohammad, R., E. Rasool, R. M. R. Modarres and B. A. Mohammad (2010) Modeling of non-Newtonian fluid flow within simplex atomizers, *in: ASME 2010 10th Biennial Conference on Engineering Systems Design and Analysis, American Society of Mechanical Engineers*, 2010, pp. 549–556.

Moon, S., C. Bae, EF. Abo-Serie and J. Choi (2007) Internal and near-nozzle flow of a pressure-swirl atomizer under varied fuel temperature. *Atomization & Sprays* 17(17), 529-550.

Pang, Y., H. Kim, Z. M. Liu and H. A. Stone (2014) A soft microchannel decreases polydispersity of droplet generation, *Lab Chip* 14, 4029–4034.

Santolaya, J. L., L. A. Aísa, E. Calvo, et al. (2010) Analysis by droplet size classes of the liquid flow structure in a pressure swirl hollow cone spray. *Chemical Engineering & Processing Process Intensification* 49(1), 125-131.

Sun, Y. B., A. M. Alkhedhair, Z. Q. Guan and K. Hoomana (2018) Numerical and experimental study on the spray characteristics of full-cone pressure swirl atomizers. *Energy* 160, 678-692

Wang, X., A. Lefebvre (2013) Atomization performance of pressure-swirl nozzles, *Atomization & Sprays* 4(3), 351-367.

Wang, X., Z. M. Liu, Y. Pang (2017) Concentration gradient generation methods based on microfluidic systems, *RSC Advances* 7, 29966-29984

Wen, S., Y. Lan, J. Zhang, S. H. Li, H. Y. Zhang and H. Xing (2016) Analysis and experiment on atomization characteristics of ultra-low-volume swirl nozzle for agricultural unmanned aviation vehicle, *Transactions of the Chinese Society of Agricultural Engineering*.

Wimmer, E., G. Brenn (2013) Viscous flow through the swirl chamber of a pressure-swirl atomizer. *International Journal of Multiphase Flow* 53(1), 100-113.

Xie, J. L., Z. W. Gan, F. Duan, T.N. Wong, S.C.M. Yu and R. Zhao (2013) Characterization of spray atomization and heat transfer of pressure swirl nozzles, *International Journal of Thermal Sciences* 68, 94-102.

Zhang, X. C., X. F. Wang (1989) Theoretical and Experimental Study on the Effect of Liquid Viscosity on Centrifugal Nozzle Spray Concentration Distribution and Spray Cone Angle. *Journal of Propulsion Technology* 10(6), 19-24.